

Received April 6, 2019, accepted April 29, 2019, date of publication May 22, 2019, date of current version June 21, 2019.

Digital Object Identifier 10.1109/ACCESS.2019.2918178

# Local Average Signal Strength Estimation for Indoor Multipath Propagation

HUTHAIFA OBEIDAT<sup>1</sup>, ALI A. S. ALABDULLAH<sup>2,3</sup>, NAZAR T. ALI<sup>4</sup>, (Senior Member, IEEE),  
RAMEEZ ASIF<sup>2</sup>, OMAR OBEIDAT<sup>5</sup>, MOHAMMED S. A. BIN-MELHA<sup>2,6</sup>, WAFSA SHUAIEB<sup>6</sup>,  
RAED A. ABD-ALHAMEED<sup>1,2,7</sup>, (Senior Member, IEEE),  
AND PETER EXCELL<sup>8</sup>, (Senior Member, IEEE)

<sup>1</sup>Faculty of Engineering, Jerash University, Jerash, Jordan

<sup>2</sup>School of Electrical Engineering and Computer Science, University of Bradford, Bradford BD7 1DP, U.K.

<sup>3</sup>College of Electronics, University of Nineveh, Mosul, Iraq

<sup>4</sup>Department of Electrical and Computer Engineering, Khalifa University, Abu Dhabi, United Arab Emirates

<sup>5</sup>College of Engineering, Wayne State University, Detroit, MI 48202, USA

<sup>6</sup>Faculty of Engineering, Omar Al-Mukhtar University, Al Bayda, Libya

<sup>7</sup>Information and Communication Engineering Department, Basrah University College of Science and Technology, Basrah 24001, Iraq

<sup>8</sup>Department of Engineering, Wrexham Glyndŵr University, Wrexham LL11 2AW, U.K.

Corresponding author: Huthaifa Obeidat (h.obeidat@jpu.edu.jo)

This work was supported in part by the Innovation Programme under Grant H2020-MSCA-ITN-2016 SECRET-722424, and in part by the U.K. Engineering and Physical Sciences Research Council (EPSRC) under Grant EP/E022936/1.

**ABSTRACT** A comprehensive study of approaches for the estimation of the local average of the received signal strength (RSS) for indoor multipath propagation is presented. The effects of the required number of the RSS data samples and the Euclidean distances between the neighboring samples are investigated over 1D, 2D, and 3D configurations. It was found that the effect of fast fading was reduced to an acceptable level using a 2D horizontal arrangement with a relatively large spacing configuration. Furthermore, averaging was enhanced with a larger spacing compared to smaller spacing when considering the same number of samples.

**INDEX TERMS** Fast fading, indoor propagation, local average RSS, localization, signal strength, WLAN.

## I. INTRODUCTION

Wireless communication engineers frequently experience difficulty with the dynamic behavior of wireless radio channels. Wireless channels are more susceptible to noise, interference and other hindrances than wired connections [1]. The challenge, therefore, is to make the channel determinable at any location.

When a signal arrives at a receiver, the signal strength level is influenced by three different scales of variations, the largest scale being path loss, which is range dependent, the signal strength level decaying approximately exponentially. The second scale is due to shadowing, where the signal strength varies around its mean according to a log-normal distribution: such variations take place over ranges of the order of  $10\lambda$ - $30\lambda$ . The smallest scale is due to multipath effects, where the signal follows a Rayleigh or Rician distribution and variations are of order  $0.5\lambda$  [2]. Multipath effects can

be observed when the mobile terminal moves distances that are short compared to the correlation shadowing distance, hence this is called small-scale fading. Due to these effects, signal strength (SS) recorded at the receiver becomes very sensitive to any small movement. In fact, even if the receiver is stationary, the recorded SS will still vary noticeably due to other influences on the path; this will make the use of SS in localization impractical and inaccurate.

Researchers have developed techniques to remove the effect of small-scale fading [3] so that the received signal strength (RSS) will be linked to path loss and shadowing only: such integrated representations can be expected to make the RSS-distance relationship more tractable. One of the main problems in localization using RSS is the non-monotonic fading of RSS level with distance and such a problem will lead to ambiguity of location estimation. For example, Fig.1 shows the RSS data along a building hallway that was simulated using *Wireless Insite*® ray tracing software: when the mobile's RSS is  $-35$  dBm, there are five possible locations for the mobile; the range of error is around 18 m which

The associate editor coordinating the review of this manuscript and approving it for publication was Xijun Wang.

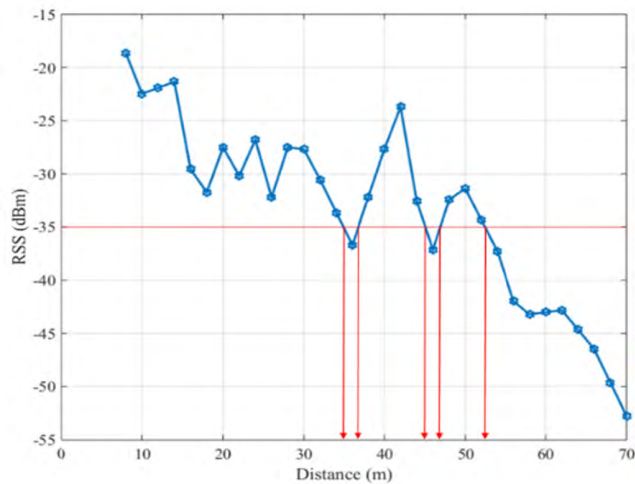


FIGURE 1. RSS-distance ambiguity problem.

is unacceptable for localization purposes in indoor environments. The primary aim is to manipulate this relationship to be unambiguous (i.e. monotonically decreasing). A possible way to achieve this is to average over local means to remove the effects of fast fading [3].

The organization of this paper is as follows: section II introduces ray tracing local averaging methods; section III presents the related literature review; in section IV methodology and the simulation setup are explained; the results and discussion are presented in section V and finally conclusions are drawn in section VI.

## II. VECTOR SUM vs. POWER SUM PREDICTION METHODS

In ray tracing techniques, there are two methods to perform averaging: the first method takes the power sum of all multipath rays, which is known as “Power sum prediction (PS)” [3]

$$\langle P_{PS} \rangle = \sum_M P_M \quad (1)$$

where  $\langle P_{PS} \rangle$ ,  $M$  and  $P_M$  are the averaged power using the PS method, number of multipath rays and power of each individual ray respectively.

The second method takes the average of the squared sum of all electric fields (amplitudes and phases): this is known as “vector sum prediction (VS)” [3]:

$$\langle P_{VS} \rangle = \left| \sum_M \sqrt{P_M} e^{-j\varphi_M} \right|^2 \quad (2)$$

where  $\langle P_{VS} \rangle$  is the averaged power using the VS method and  $\varphi_M$  is the  $M^{\text{th}}$  ray phase in radians.

In [4] PS is recommended to be used for frequencies higher than 2 GHz, while VS is recommended for lower frequencies. In [3] the PS method is said to be quicker and better; however, it is hard to implement in practice as it requires the receiver to be capable of distinguishing all incoming rays so that the effect of each ray’s phase will be removed; this process

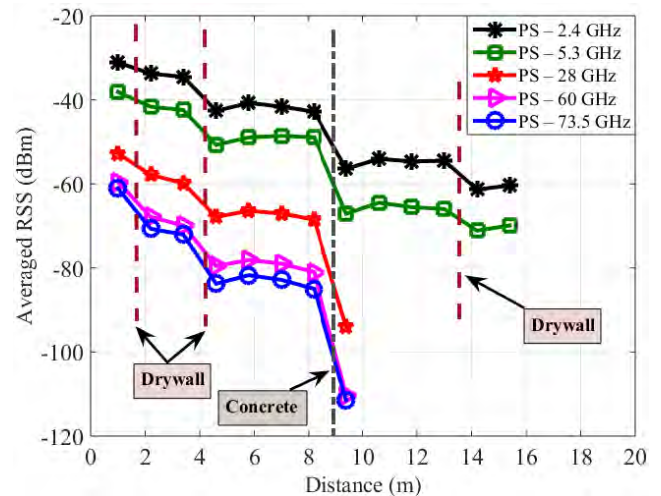


FIGURE 2. PS method performance for a range of frequencies.

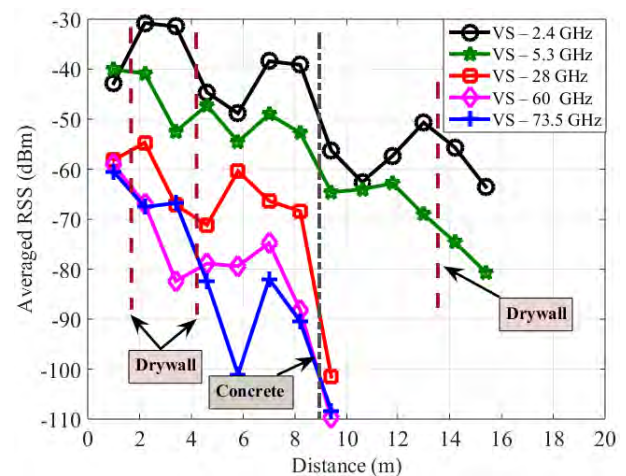


FIGURE 3. VS method performance for a range of frequencies.

requires a very large array antenna to detect arrival angles and it also requires very large bandwidth to detect delays.

The performance of the above methods was investigated over a set of frequencies, including 2.4 GHz, 5.3 GHz, 28 GHz, 60 GHz and 73.5 GHz: simulation results are presented in Fig. 2 and Fig. 3. It can be seen that averaged RSS using the PS method tends to be similar for all frequencies since this method removes the effect of multipath fading so that the only contributors to SS level are the path loss and shadowing. The reason why these averaged RSS curves take the form of similar layers is due to two types of losses: path loss with distance and wall losses, both of which are frequency dependent. On the other hand; The VS method takes into account phase information in estimation of the RSS averaged value. However, due to the presence of many multipath components, where each one has a different phase, the RSS averaged value will have large variations when the position of the receiver is slightly changed, especially at higher frequencies; This will make the SS-distance relationship less likely to be monotonic and therefore will reduce the localization efficacy.

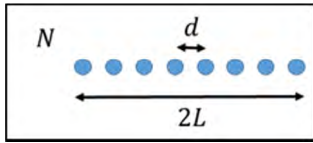


FIGURE 4. Averaging length, spacing and number of samples.

In this paper, the investigated frequency is limited to the 2.4 GHz band only: investigation of further frequencies will be the subject of a forthcoming paper.

### III. PREVIOUS RELATED WORK

In averaging estimation process three parameters are considered, as shown in Fig. 4 [5]: the averaging length ( $2L$  - also known as window size); the number of samples ( $N$  - also known as the number of collection points) and the distance between the samples ( $d$  - also known as spacing). Finding two parameters is sufficient to find the third using the relation  $2L = Nd$ . In a study conducted by [6] over the band 1.8 to 5.2 GHz the window size was found to be equal to 1 m or ( $5\lambda$ - $15\lambda$ ), where the corresponding variance of the estimated local mean signal was around 1 dB [7]. By having a sufficient number of samples the estimated variance will be reduced [8].

A set of measurements was conducted by the authors of [3] at 0.9 and 2.4 GHz and averaging was performed. Two procedures were followed: in the first procedure, many measurements were taken on circular paths around the point of interest, also known as the reference point (RP), then averaging was performed: each circular path had a 0.3 m radius and measurements were taken from 120 points on the circle; the whole process being repeated every 0.6 m.

In the second method, measurements were collected from many points lying on a linear path, where the spacing between the measurement points was  $\lambda/4$  and averaging was performed over a window size of  $10\lambda$ . This method was claimed to be appropriate for LOS and measurements in corridors [3]. In [9] the authors performed RSS averaging over regions of dimensions  $(2\lambda)^2$ . In [10] averaging was performed over regions of dimensions  $(3\lambda)^2$ , while in [11] and [12] the regions were of size  $(3\lambda)^3$ . In [13] averaging was conducted over a  $10\lambda$  interval while the minimum spacing between samples was set to  $0.38\lambda$ .

Averaging should not distort the effect of large-scale fading; therefore, estimating correlation distance  $r_c$  is crucial and this can be determined by estimating  $1/e$  of the normalized shadowing autocorrelation  $\rho_s$ . The autocorrelation function is a function of location variability  $\sigma_L$  which is in turn a function of frequency [14].  $\sigma_L$  tends to increase as frequency increases; therefore, for larger frequencies  $\rho_s$  decreases and hence  $r_c$  decreases. In [15] the authors considered the shadowing correlation distance to be in the range of 1-2 m, as estimated by [16]: they found that using a  $10\lambda$  spacing window would be too long while using  $4\lambda$  would be optimum.

In [17], the authors generalized the Lee model to include different propagation environments, including urban, suburban, rural and indoor environments with the UHF band.

They recommended the window size  $2L$  to be  $5\lambda$ - $10\lambda$  for indoor environments.

In [18] an analysis is reported that aimed to find the best averaging window and spacing; it was found that the best averaging window was within the range  $20\lambda$ - $40\lambda$  with a sample spacing of  $1.11\lambda$  (36 samples) to ensure that samples were uncorrelated. This procedure was also applied for indoor application at 15 GHz [19]. Work done by [18] was generalized for the medium-frequency band [20]: they found that the best window size was  $2\lambda$ , the optimum distance between samples was  $0.17\lambda$  and the best number of samples was 8.

In [21] averaging over a window size of  $40\lambda$  was performed at 15 GHz in indoor corridor scenarios in order to obtain small-scale fading characteristics. In [22] a local mean was taken over a rectangular area of  $(0.1 \text{ m})^2$  at 1.8 GHz, where nine measurements were taken within the grid.

For Nakagami propagation channels it is recommended by [7] to use 40 collection points within a  $20\lambda$  averaging window for channels with a small number of multiple paths:  $2 \leq m < 4$  ( $m$  is the fading parameter), while for multipath channels in the range  $4 \leq m \leq 8$  it was recommended to use 20 collection points within a  $10\lambda$  averaging window. On the other hand, for channels with a higher number of multiple paths as compared to the Rayleigh case, it was recommended to use  $0.5\lambda$  spacing between collection points within a  $90\lambda$  averaging window. In [23] local mean estimation was conducted in a multi-floor building; measurements were collected through routes in the environment: these environments were gridded and then a local mean was estimated. The sizes of these grids were  $(k\lambda \times k\lambda)$ , where  $k$  ranged from 1 to 15; measurements were conducted at 0.9 GHz and 1.9 GHz.

At 0.9 GHz  $k$  was in the range of 6.5 to 7.0, while at 1.9 GHz it was in the range from 5.0 to 12.5. The performance was compared to the results in [18], however, neither approach outperformed the other. In [18] the authors assumed a normal distribution for SS while in [24] the SS distribution was found to be left-skewed: skewness is due to the limitation on the maximum achievable RSS at each location.

In [25] the authors conducted simulations of the estimation of the electric field strength at 3 GHz and 5 GHz, using the FDTD method. It was found that averaging over a 3D volume, a cube with a side length of  $3.3\lambda$ , showed agreement between the local mean magnitude of the simulation and the theoretical electric field. Measurements and simulation were conducted at 3 GHz and it was found that as the averaging volume increased the error of estimating the electric field decreased.

Averaging at 900 MHz over  $20\lambda$  was reported in [26]: the approach was applied in indoor environments in circumstances where either end of the radio link is moving.

### IV. METHODOLOGY AND SIMULATION SETUP

In practice, in order to use the PS method, the receiver should possess ultra-wideband bandwidth in order to be able to distinguish the closed multipath; also the receiver should use a large antenna array to detect all angle of arrival signals.

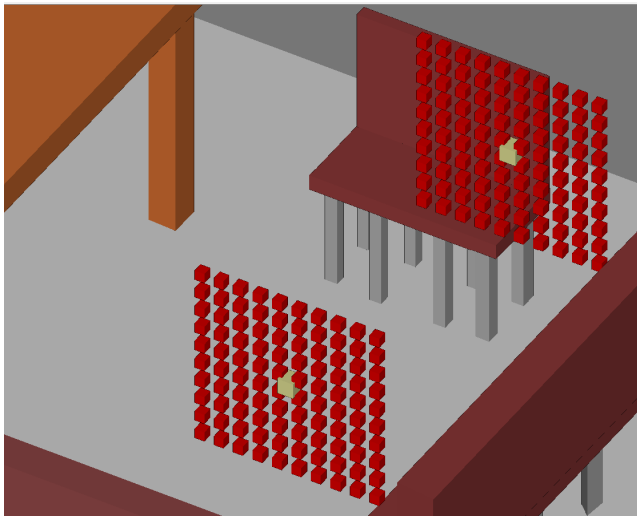


FIGURE 5. Exemplar SS collection points: Red points for averaging, yellow points are the points of interest.

Due to the difficulty of satisfying such requirements in all receivers, ray tracers are used as they provide information about the multipath propagation channel, including its corresponding received signal strength, phases, angles of arrival and departure, and time of arrivals. Therefore, the PS method can be used and the averaged value using the PS method will serve as a reference. Where the performance of different types of configurations that apply the VS method is compared to the reference, the one with the closest performance to the PS method can be deemed to be the best configuration.

Although PS is more accurate than VS, VS is easier to apply, therefore collecting samples (each using VS) and then performing local averaging will enhance the results to be better than those from VS but with less complexity than PS. In the present work, different simulated configurations were used to estimate the averaged RSS using the VS method.

In the simple scenario of the two-ray ground-reflection model, there will be a direct ray and a ground-reflected ray. The two paths have different lengths and hence different phases; thus for a moving terminal, the received power will follow constructive and destructive interference every phase difference of  $\pi$ , representing a path difference of  $\lambda/2$ . If the signals are coming from opposite directions, then a moving terminal experiences constructive and destructive interference every phase difference of  $\pi/2$ , representing a path difference of  $\lambda/4$ . In general, if signals are coming from different directions then a moving terminal experiences constructive and destructive interference within the range of  $\lambda/2$  to  $\lambda/4$ . In real life scenarios, multiple paths tend to be more than two; however, the same concept still applies, therefore, the present work started by averaging over  $\lambda/4$ , and then the arrangement size was increased by  $\lambda/4$  increments each time.

As seen in Fig. 5, the objective is to remove the effect of fast fading from the collected signal strength (SS), therefore a group of collection points (red cubes in the figure) are taken around the point of interest (yellow cubes) and then the

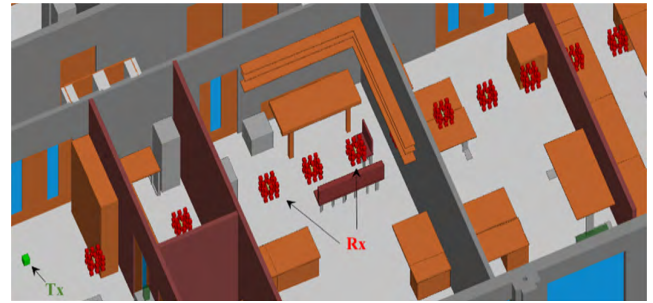


FIGURE 6. Example of a scenario conducted in the Wireless InSite model.

TABLE 1. Wireless insite settings for the investigated scenario.

Property	Setting
Number of reflections	6
Number of transmissions	4
Number of diffractions	1
Number of reflections before the first diffraction	3
Number of reflections after the last diffraction	3
Number of reflections between diffractions	1
Number of transmissions before the first diffraction	2
Number of transmissions after the last diffraction	2
Number of transmissions between diffractions	1
Ray tracing method	SBR
Propagation model	Full 3D

corresponding RSS values at the red points are averaged. The averaging process requires conversion of RSS values from the dB scale to linear scale, followed by averaging and then conversion back to dB.

The simulation was conducted using the ray-tracing software *Wireless Insite*®, which has been extensively validated, especially over the UHF band [27] and over 802.11ac frequencies [28], [29]. The operating frequency used in these simulations was 2.45 GHz and the distance between points of interest (yellow points) was  $10\lambda$  as this has been reported to give the optimum representative data [18]. Fig. 6 shows an example of a scenario conducted in the Wireless InSite software where different positions in different rooms are evaluated. Wireless Insite settings for these simulations are listed in Table 1, where SBR stands for Shooting-and-Bouncing-Rays.

Simulations were conducted in a simulated environment for the third floor of a typical modern office-type building (the Chesham Building at the University of Bradford, U.K.). As seen in Fig. 7, the model considered different types of materials used in the building: these materials have frequency dependent properties [30] and therefore, their corresponding electrical parameters (relative permittivity  $\epsilon_r$  and conductivity  $\sigma$ ) will change as frequency changes. Typical values for  $\epsilon_r$  and  $\sigma$  are given in Table 2: these were calculated using eqns. (3) and (4), where  $\alpha$ ,  $\beta$  and  $\gamma$  are given in [30].

$$\sigma = \alpha f_{GHz}^{\beta} S/m \tag{3}$$

$$\epsilon_r = \rho f_{GHz}^{\gamma} \tag{4}$$

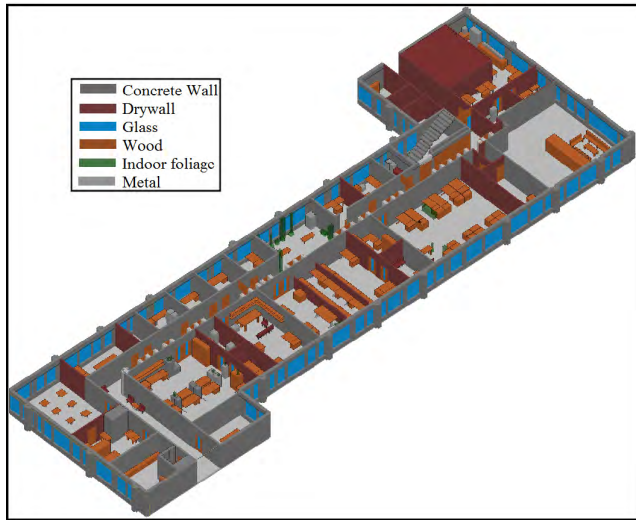


FIGURE 7. Simulated Environment for the 3rd floor of the Chesham Building, University of Bradford.

TABLE 2. Material properties adopted, for frequency 2.45 GHz.

Material	$\epsilon_r$	$\sigma$
Concrete	5.31	0.0663
Glass	6.27	0.0122
Wood	1.99	0.012
Drywall	2.94	0.0216
Wet Ground	30	0.4681

The use of ray tracing software will reduce the effort, time and cost required to perform the experiment; however, without careful consideration of the software settings, the observed results will be pessimistic or underestimated. The simulated results in the indoor environment are also highly dependent on material properties and therefore, precise values for material conductivity and permittivity were chosen from research papers published in respected journals and with a high score of citations.

In this discussion, three parameters are considered: arrangement size, arrangement type and the distance between the collection points (spacing). The total number of scenarios investigated was 406.

**A. ARRANGEMENT TYPES**

The word *arrangement* refers to the configuration of the overall set of collection points. The shape of the overall set of collection points is termed the *arrangement type*, while the dimensions of this configuration are termed the *arrangement size*. In this analysis, different types of arrangement have been studied to validate the best one for averaging. Seven arrangement types have been studied, a three-dimensional arrangement (3D), a two-dimensional arrangement where the collection points lie on a plane horizontal to the floor (2D-H), a two dimensional arrangement where the collection points lie on a plane perpendicular to the floor (2D-V), a one-dimensional arrangement perpendicular to the floor (1D-V), a one-dimensional arrangement perpendicular to the line

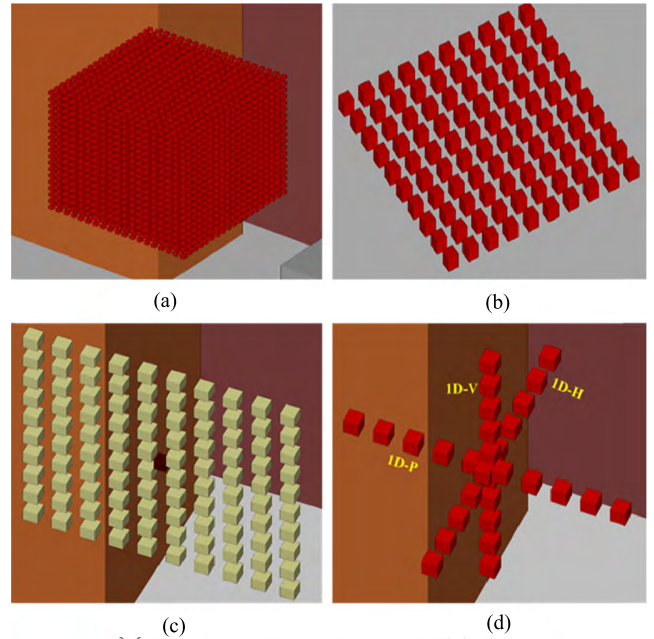


FIGURE 8. Arrangement types used in the simulation. (a) 3D. (b) 2D-H. (c) 2D-V. (d) HYB.

joining the points of interest and horizontal to the floor (1D-P), a one-dimensional arrangement parallel (horizontal) to both the line joining the points of interest and the floor (1D-H) and a combination of all one-dimensional averaging loci, termed as hybrid (HYB). In all tested scenarios the collection points were equally spaced: see Fig. 8

In the 3D arrangement, a set of measurements was taken with equal spacing, forming a cube as seen in Fig. 8a, where the point of interest is at the center of this cube. For example, a  $(4.5\lambda)^3$  arrangement is a cube with edge length  $4.5\lambda$ . For both 2D-H and 2D-V, the collection points form a square which is concentric with the point of interest, as seen in Fig. 8b and 8c. The 1D-H, 1D-P, 1D-V and HYB are symmetrical about the point of interest, as seen in Fig. 8-d.

**B. ARRANGEMENT SIZE**

Different arrangement sizes have been investigated, from  $0.25\lambda$  up to  $4.5\lambda$  with  $0.25\lambda$  incremental steps.

**C. SPACING BETWEEN POINTS**

Initially, for each arrangement size, the spacing between the adjacent points was set to be  $0.25\lambda$ ; then, in order to investigate the effect of spacing between points, the spacing was increased by an increment of  $0.25\lambda$  each time (i.e. Spacings:  $0.25\lambda, 0.5\lambda, 0.75\lambda \dots$  up to maximum arrangement size). However, not all arrangement sizes can maintain the same size when the spacing is increased (for example, if the spacing for the  $4.25\lambda$  size were incremented by  $0.5\lambda$  then the resultant arrangement would be either  $4.5\lambda$  or  $4\lambda$ ; therefore, spacing by this increment cannot be used). Table 3 lists the arrangement sizes used in the simulations along with arrangement types and their possible spacings; the table also shows the number

**TABLE 3.** Arrangement sizes and their possible spacings, with the required number of points for averaging.

	Size	Spacing	3D	2D-H	2D-V	1D-H	1D-V	1D-P	HYB
1	4.5λ	0.25λ	6859	361	361	19	19	19	57
2		0.5λ	1000	100	100	10	10	10	30
3		0.75λ	343	49	49	7	7	7	21
4		1.5λ	64	16	16	4	4	4	12
5		2.25λ	27	9	9	3	3	3	9
6		4.5λ	8	4	4	2	2	2	6
7	4.25λ	0.25λ	5832	324	324	18	18	18	54
8		4.25λ	8	4	4	2	2	2	6
9	4λ	0.25λ	4913	289	289	17	17	17	51
10		0.5λ	729	81	81	9	9	9	27
11		λ	125	25	25	5	5	5	15
12		2λ	27	9	9	3	3	3	9
13		4λ	8	4	4	2	2	2	6
14	3.75λ	0.25λ	4096	256	256	16	16	16	48
15		0.75λ	216	36	36	6	6	6	18
16		1.25λ	64	16	16	4	4	4	12
17		3.75λ	8	4	4	2	2	2	6
18	3.5λ	0.25λ	3375	225	225	15	15	15	45
19		0.5λ	512	64	64	8	8	8	24
20		1.75λ	27	9	9	3	3	3	9
21		3.5λ	8	4	4	2	2	2	6
22	3.25λ	0.25λ	2744	196	196	14	14	14	42
23		3.25λ	8	4	4	2	2	2	6
24	3λ	0.25λ	2197	169	169	13	13	13	39
25		0.5λ	343	49	49	7	7	7	21
26		0.75λ	125	25	25	5	5	5	15
27		λ	64	16	16	4	4	4	12
28		1.5λ	27	9	9	3	3	3	9
29		3λ	8	4	4	2	2	2	6
30	2.75λ	0.25λ	1728	144	144	12	12	12	36
31		2.75λ	8	4	4	2	2	2	6
32	2.5λ	0.25λ	1331	121	121	11	11	11	33
33		0.5λ	216	36	36	6	6	6	18
34		1.25λ	27	9	9	3	3	3	9
35		2.5λ	8	4	4	2	2	2	6
36	2.25λ	0.25λ	1000	100	100	10	10	10	30
37		0.75λ	64	16	16	4	4	4	12
38		2.25λ	8	4	4	2	2	2	6
39	2λ	0.25λ	729	81	81	9	9	9	27
40		0.5λ	125	25	25	5	5	5	15
41		λ	27	9	9	3	3	3	9
42		2λ	8	4	4	2	2	2	6
43	1.75λ	0.25λ	512	64	64	8	8	8	24
44		1.75λ	8	4	4	2	2	2	6
45	1.5λ	0.25λ	343	49	49	7	7	7	21
46		0.5λ	64	16	16	4	4	4	12
47		0.75λ	27	9	9	3	3	3	9
48		1.5λ	8	4	4	2	2	2	6
49	1.25λ	0.25λ	216	36	36	6	6	6	18
50		1.25λ	8	4	4	2	2	2	6
51	λ	0.25λ	125	25	25	5	5	5	15
52		0.5λ	27	9	9	3	3	3	9
53		λ	8	4	4	2	2	2	6
54	0.75λ	0.25λ	64	16	16	4	4	4	12
55		0.75λ	8	4	4	2	2	2	6
56	0.5λ	0.25λ	27	9	9	3	3	3	9
57		0.5λ	8	4	4	2	2	2	6
58	0.25λ	0.25λ	8	4	4	2	2	2	6

of points required for averaging for all 406 scenarios. Omni-directional antennas were implemented for both transmitters and receivers.

As seen in the table, using a 3D arrangement with a size of 4.5λ and spacing of 0.25λ will be computationally expensive as it requires 6859 collection points for averaging. This is the most extreme case, but in this analysis, the aim is to find the best arrangement type, size and spacing for estimating the local mean of RSS.

**V. RESULTS AND DISCUSSIONS**

The root mean square error (RMSE) is used as a performance metric. It is taken between each scenario (vector sum) and the

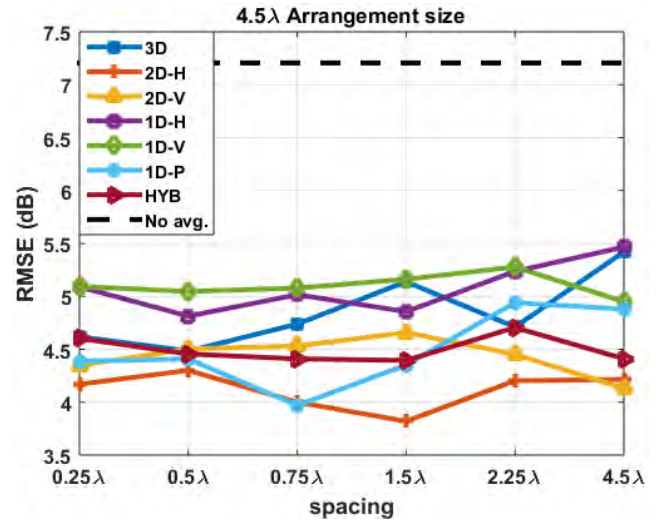


**FIGURE 9.** 4.5λ arrangement averaging (RMSE = r.m.s. error).

reference case (power sum); therefore, there are 406 RMSE results. It is worth mentioning that the smaller the RMSE between the averaged result and the power sum result, the better is the averaging performance. In other words, the aim is to have an averaged value as close as possible to the power sum method result.

**A. ARRANGEMENT SIZE**

Averaging over each arrangement size and type, and its behavior with different spacings between collection points was examined: examples of the results are presented and general observations on the analyses for all arrangements are presented after these examples.

Fig. 9 presents averaging over a 4.5λ arrangement size for all types and all possible spacings (0.25λ, 0.5λ, 0.75λ, 1.5λ, 2.25λ and 4.5λ). As seen in Table 3, the number of points used ranged from 6859 in the 3D/0.25λ (arrangement type/spacing) case to 2 points in the 1D/4.5λ cases. In the figure, it can be seen that using simpler arrangement types gives better results compared to the computationally demanding 3D cases. Averaging over a huge number of points as in the 3D/0.25λ case does not provide significant reduction of fast fading; increasing the number of points does not necessarily improve the result. Generally, the results obtained from the 3D arrangement are not satisfactory, because 3D arrangements use many points with different heights, thus many of them will examine different multipath rays, and hence the averaged value will be different from the power sum result.

As seen in the figure, all averaging results show enhancement compared to the no-averaging case (single measurement per location). For this arrangement size, the best arrangement type performance is 2D-H/1.5λ as it has the lowest RMSE; further, it requires only 16 collection points for averaging. The descending order of RMSE performance for all arrangement types is 2D-H, 2D-V, 1D-P, HYB, 3D, 1D-H and 1D-V.

Averaging over 0.25λ arrangement size is presented in Fig. 10: the number of SS collection points ranged from

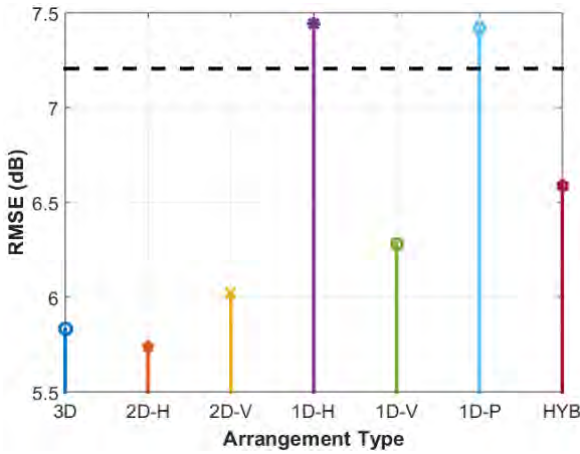


FIGURE 10.  $0.25\lambda$  arrangement averaging.

TABLE 4. Ten best arrangement results.

Arrang. type	Arrang. size/Spacing	No. of points	RMSE			
			No averaging	7.205	5.46	7.239
2D-H	1.25λ/1.25λ	4	3.525	4.308	3.230	3.769
2D-H	1.5λ/1.5λ	4	3.699	3.479	2.764	2.833
2D-H	4.5λ/1.5λ	16	3.82	2.54	3.697	3.330
2D-H	3.5λ/1.75λ	9	3.831	2.619	2.429	3.042
2D-H	3.75λ/0.25λ	256	3.835	2.436	2.787	2.660
2D-H	1.5λ/0.75λ	9	3.946	2.496	2.103	3.873
1D-P	4.5λ/0.75λ	7	3.970	2.439	2.940	3.178
2D-H	4.5λ/0.75λ	49	3.999	2.148	3.176	2.952
HYB	3.75λ/3.75λ	6	4.009	2.293	3.665	2.714
2D-H	1.75λ/0.25λ	64	4.069	2.799	2.331	2.598

eight to two, as seen in Table 3. All arrangements have poor performance as their RMSE values are more than 5.5 dB; however, 1D-H and 1D-P have results that are worse than the no-averaging case. It can be concluded that averaging with this arrangement size is not recommended.

Table 4 shows the ten best averaging results found in the whole experiment; the first RMSE column represents the ten best averaging arrangements, eight of them are of the 2D-H type. Among the top 20 arrangements, 13 are 2D-H and among the best 50 arrangements, 26 are 2D-H. On the other hand, the 2D-H arrangement type had only 4 poor results amongst the worst 100 results. Therefore, it is very plausible to recommend that this arrangement type is used for averaging. As seen in the table the best two arrangements have only four points each: although this appears promising, making a general conclusion from these results would be premature and thus a need for more trials was indicated. Therefore, the best 10 arrangements were examined in more environments in order to study more generalized results. The scenarios included LOS (propagation along a corridor) and NLOS (propagation through rooms with different antenna heights).

It was observed that the best overall performance was 2D-H  $3.75\lambda/0.25\lambda$ , this observation is rational as many points were used for averaging; however, using 256 points is very demanding in time and effort. The second-best performance was 2D-H  $1.75\lambda/0.25\lambda$  where 64 points are used, while the

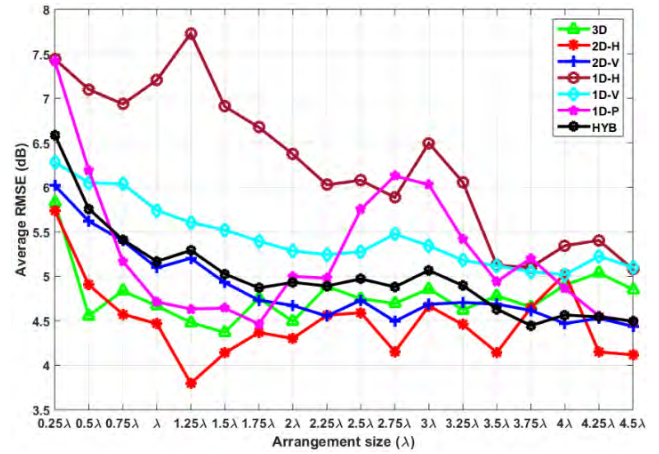


FIGURE 11. Averaged RMSE for the investigated arrangement types at all spacings for each arrangement size.

third-best performance was 2D-H  $3.5\lambda/1.75\lambda$  which needs only 9 points: this arrangement has acceptable performance and requires much less computation, thus it is recommended to be used.

An interesting observation was noted, in that the worst performances were for 2D-H  $1.25\lambda/1.25\lambda$  and 2D-H  $1.5\lambda/1.5\lambda$ , this indicates that using only four points for averaging is not recommended.

Another interesting observation is the case of the LOS scenario: as shown in the table, RMSE for no averaging (2.854 dB) tends to be very similar to the averaging results. This is presumed to be a consequence of the fact that the resultant RSS with no averaging depends on the LOS component, as the latter is the dominant path, whereas the multipath components will not affect the main path reading. Therefore, averaging in LOS scenarios will not enhance RSS readings, provided that the transmitter and receiver antennas are omnidirectional.

A comparison between arrangement type performances for all spacings with each arrangement size is presented in Fig.11. 2D-H has the best overall performance for almost all of the arrangement sizes and this result can be explained as the width of the floor is likely to be larger than its height, therefore, most of the reflections (which contribute toward the fading effects) are thus occurring on the horizontal plane. It can be seen also that both 2D-H and 3D performances were not enhanced significantly after a certain size; hence it may be better to use arrangements with a smaller size as they need fewer points. The descending order of performance for all arrangement types and for all arrangement sizes is seen to be 2D-H, 3D, 2D-V, HYB, 1D-P, 1D-V then 1D-H.

In Fig. 11, the overall performance for 1D and HYB arrangement types for all spacings and all arrangement sizes is presented. 1D-H has the worst performance for the majority of the examined sizes, while the HYB tends to have the best performance for the majority of the arrangement sizes. Although HYB shows better performance in general, averaging with the 1D-P arrangement tends to have the lowest

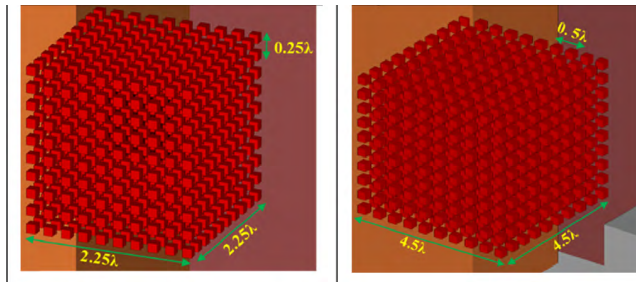


FIGURE 12. Example of arrangements  $(2.25\lambda/0.25\lambda)$  and  $(4.5\lambda/0.5\lambda)$  which have the same number of points but different spacing.

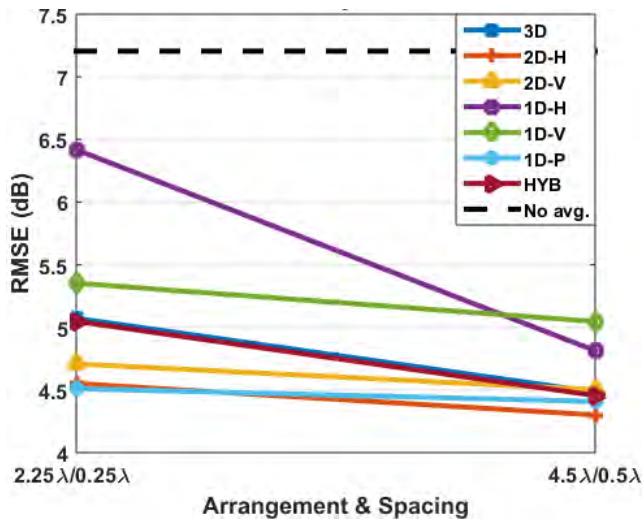


FIGURE 13. Performance comparison for arrangements with 10 layers of data collection points.

average RMSE for arrangement sizes from  $0.75\lambda$  to  $2\lambda$ ; therefore, it may be better to use this arrangement type as it needs a lower number of collection points. It should be noted that these values are averaged over all spacings, therefore when choosing any arrangement type for averaging it is recommended to check the individual averaging result for each spacing with each arrangement size.

**B. NUMBER OF POINTS**

Several arrangement configurations have the same number of collection points, for example, arrangement types employing  $4.5\lambda/0.5\lambda$  and  $2.25\lambda/0.25\lambda$  have the same number of points (see Table 3 and Fig. 12). The aim of this part of the study was to find the optimum spacing for the same number of points.

Data in Table 3 rows 2 and 36 are presented in Fig. 13, these data have the same number of points but, by increasing the spacing between the points, the RMSE tends to decrease as the RMSE was reduced by 0.6 dB

Fixing the number of points and changing the spacing does not improve the 3D and 2D-H results significantly but it gives improvement for 2D-V, 1D-V, 1D-H and HYB, and in some cases 1D-P also shows a better performance.

**C. ARRANGEMENT TYPE**

Since 2D-H gives the best results it is worthwhile to investigate this arrangement’s relationship with spacing and size and

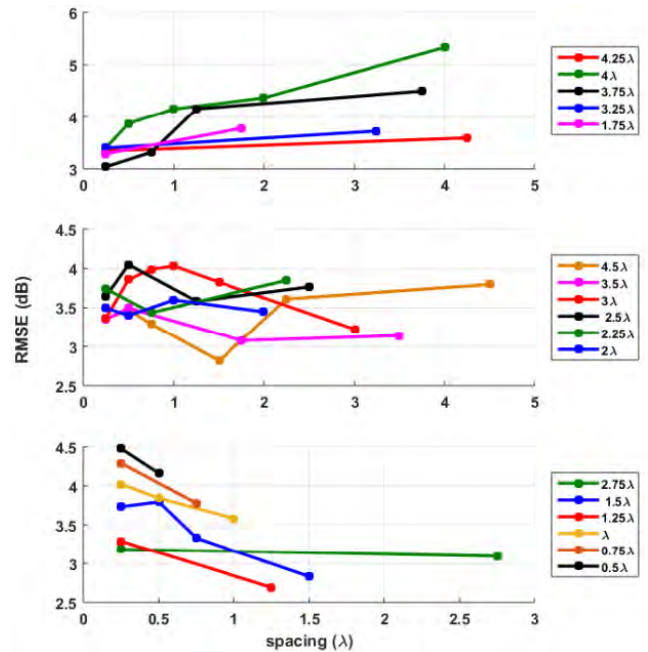


FIGURE 14. RMSE relationship with spacing for the 2D-H arrangement type.

its effect on RMSE. Fig. 14 presents the RMSE relationship with spacing for the 2D-H arrangement type for all arrangement sizes. It was found that for small arrangement sizes ( $\leq 1.5\lambda$ ) RMSE decreases as spacing increases. For large ( $\geq 3.25\lambda$ ) and medium arrangement sizes no significant spacing relationship between spacing and RMSE was found, therefore it can be recommended to use the 2D-H arrangement with smaller size and larger spacing.

Generally, for the 3D, 2D-H, 1D-V and 1D-P arrangements, smaller arrangement sizes give better results as spacing increases. The 2D-V and 1D-H type have better results for large arrangement sizes as spacing increases. The 1D-V type has better results for most medium arrangement sizes as spacing increases. The HYB type tends to have good results as spacing increases for most of the arrangement sizes.

**VI. CONCLUSIONS**

In this paper a set of comprehensive studies on estimation of local average signal strength for indoor multipath propagation was conducted, covering 406 tested scenarios in a typical modern office-type building. The work investigated the importance of averaging and its effect on localization. The set of results indicated the best-performing arrangement types, the effect of changing sample spacing for the same number of samples, and the relationship between arrangement type and spacing for all arrangement sizes. It was found that using a horizontal two-dimensional configuration of samples reduces the effect of fast fading significantly; also, using the same number of samples with larger spacing enhanced averaging compared to small spacings. The use of larger configurations improves averaging for some arrangement types while it does not improve it for others. Smaller arrangement sizes



demonstrated better results as spacing was increased for the cases of the 3D, 2D-H, 1D-V and 1D-P arrangement types, while the HYB type gave good results as spacing increased for most of the arrangements.

The results suggest the use of a grid size larger than  $0.75\lambda$  as the RMSE tends to be less than for the smaller arrangement sizes. Arrangements with at least 9 points may be an optimum choice as they provide good results and require manageable numbers of collection points.

## ACKNOWLEDGMENT

The authors acknowledge the financial support from the Innovation Programme under Grant H2020-MSCA-ITN-2016 SECRET-722424 and by the U.K. Engineering and Physical Sciences Research Council (EPSRC) under Grant EP/E022936/1.

## REFERENCES

- [1] A. Goldsmith, *Wireless Communications*. Cambridge, U.K.: Cambridge Univ. Press, 2005.
- [2] G. L. Turin, F. D. Clapp, T. L. Johnston, S. B. Fine, and D. Lavry, "A statistical model of urban multipath propagation," *IEEE Trans. Veh. Technol.*, vol. 21, no. 1, pp. 1–9, Feb. 1972.
- [3] R. A. Valenzuela, O. Landron, and D. L. Jacobs, "Estimating local mean signal strength of indoor multipath propagation," *IEEE Trans. Veh. Technol.*, vol. 46, no. 1, pp. 203–212, Feb. 1997.
- [4] V. Erceg, A. J. Rustako, and R. Roman, "Diffraction around corners and its effects on the microcell coverage area in urban and suburban environments at 900 MHz, 2 GHz, and 4 GHz," *IEEE Trans. Veh. Technol.*, vol. 43, no. 3, pp. 762–766, Aug. 1994.
- [5] P. Njemcevic and V. Lipovac, "Estimation of radio signal spatial local mean," in *Proc. 24th Int. Conf. Softw., Telecommun. Comput. Netw. (SoftCOM)*, Sep. 2016, pp. 1–5.
- [6] P. Njemcevic, "A novel approach in determination of the appropriate spatial averaging signal length," *Wireless Pers. Commun.*, vol. 82, pp. 1851–1861, Jun. 2015.
- [7] N. Pamela, "Local average signal estimation in Nakagami-m channels," in *Proc. 6th Int. Symp. Commun., Control Signal Process. (ISCCSP)*, May 2014, pp. 441–444.
- [8] B. Ai, Z. D. Zhong, G. Zhu, and M. Zhao, "Novel statistical criteria for local mean power estimation in wireless coverage prediction," *IET Microw. Antennas Propag.*, vol. 5, no. 5, pp. 596–604, Apr. 2011.
- [9] A. C. Austin, "Wireless channel characterization in burning buildings over 100–1000 MHz," *IEEE Trans. Antennas Propag.*, vol. 64, no. 7, pp. 3265–3269, Jul. 2016.
- [10] A. C. M. Austin, N. Sood, J. Siu, and C. D. Sarris, "Application of polynomial chaos to quantify uncertainty in deterministic channel models," *IEEE Trans. Antennas Propag.*, vol. 61, no. 11, pp. 5754–5761, Nov. 2013.
- [11] A. C. Austin, "Performance estimation for indoor wireless systems using FDTD method," *Electron. Lett.*, vol. 51, pp. 1376–1378, Aug. 2015.
- [12] A. C. M. Austin, M. J. Neve, and G. B. Rowe, "Modeling propagation in multifloor buildings using the FDTD method," *IEEE Trans. Antennas Propag.*, vol. 59, no. 11, pp. 4239–4246, Nov. 2011.
- [13] M. Lindh , K. H. Johansson, and A. Bicch, "An experimental study of exploiting multipath fading for robot communications," in *Proc. 3rd Int. Conf. Robot. Sci. Syst.*, Jun. 2007, pp. 289–296.
- [14] S. Saunders and A. Arag n-Zavala, *Antennas and Propagation for Wireless Communication Systems*, 2nd ed. Hoboken, NJ, USA: Wiley, 2007.
- [15] I. Dey, G. G. Messier, and S. Magierowski, "Joint fading and shadowing model for large office indoor WLAN environments," *IEEE Trans. Antennas Propag.*, vol. 62, no. 4, pp. 2209–2222, Apr. 2014.
- [16] N. Jalden, P. Zetterberg, B. Ottersten, A. Hong, and R. Thoma, "Correlation properties of large scale fading based on indoor measurements," in *Proc. IEEE Wireless Commun. Netw. Conf.*, Mar. 2007, pp. 1894–1899.
- [17] P. Njemcevic, A. Lipovac, and V. Lipovac, "Improved model for estimation of spatial averaging path length," *Wireless Commun. Mobile Comput.*, vol. 2018, May 2018, Art. no. 4704218.
- [18] W. C. Y. Lee, "Estimate of local average power of a mobile radio signal," *IEEE Trans. Veh. Technol.*, vol. 34, no. 1, pp. 22–27, Feb. 1985.
- [19] Q. Wang, B. Ai, K. Guan, D. W. Matolak, R. He, and X. Zhou, "Ray-based statistical propagation modeling for indoor corridor scenarios at 15 GHz," *Int. J. Antennas Propag.*, vol. 2016, Mar. 2016, Art. no. 2523913.
- [20] D. de la Vega, S. Lopez, J. M. Matias, U. Gil, I. Pena, M. M. Velez, J. L. Ordiales, and P. Angueira, "Generalization of the lee method for the analysis of the signal variability," *IEEE Trans. Veh. Technol.*, vol. 58, no. 2, pp. 506–516, Feb. 2009.
- [21] Q. Wang, B. Ai, K. Guan, Y. Li, and Z. Zhong, "Ray-based analysis of small-scale fading for indoor corridor scenarios at 15 GHz," in *Proc. Asia-Pacific Symp. Electromagn. Compat. (APEMC)*, May 2015, pp. 181–184.
- [22] I. Marinovic, and D. Coko, "Inter-floor wide band radio channel measurements and simulation applying Saleh-Valenzuela model," *Automatika*, vol. 56, pp. 91–99, Jan. 2015.
- [23] J. Sese a-Osorio, I. Zaldivar-Huerta, and A. Arag n-Zavala, "Experimental estimation of the large-scale fading in an indoor environment and its impact on the planning of wireless networks," in *Proc. Int. Microw. Optoelectron. Conf. (IMOC)*, Aug. 2013, pp. 1–5.
- [24] K. Kaemarungsi and P. Krishnamurthy, "Properties of indoor received signal strength for WLAN location fingerprinting," in *Proc. 1st Annu. Int. Conf. Mobile Ubiquitous Syst., Netw. Services*, Aug. 2004, pp. 14–23.
- [25] S. S. Zhekov, O. Franek, and G. F. Pedersen, "Numerical modeling of indoor propagation using FDTD method with spatial averaging," *IEEE Trans. Veh. Technol.*, vol. 67, no. 9, pp. 7984–7993, Sep. 2018.
- [26] W. Honcharenko, H. L. Bertoni, and J. L. Dailing, "Bilateral averaging over receiving and transmitting areas for accurate measurements of sector average signal strength inside buildings," *IEEE Trans. Antennas Propag.*, vol. 43, no. 5, pp. 508–512, May 1995.
- [27] P. Mededovic, M. Veletic, and Z. Blagojevic, "Wireless insite software verification via analysis and comparison of simulation and measurement results," in *Proc. 35th Int. Conv. MIPRO*, May 2012, pp. 776–781.
- [28] Y. A. S. Dama, R. A. Abd-Alhameed, F. Salazar-Quinonez, S. M. R. Jones, and J. G. Gardiner, "Indoor channel measurement and prediction for 802.11 n system," in *Proc. IEEE Veh. Technol. Conf. (VTC Fall)*, Sep. 2011, pp. 1–5.
- [29] Z. Yun and M. F. Iskander, "Ray tracing for radio propagation modeling: Principles and applications," *IEEE Access*, vol. 3, pp. 1089–1100, 2015.
- [30] *Propagation Data and Prediction Methods for the Planning of Indoor Radiocommunication Systems and Radio Local Area Networks in the Frequency Range 900 MHz to 100 GHz*, document Rec. ITU-R P.1238-7, ITU, Geneva, Switzerland, 2012.



He has been a member of the Jordanian Engineering Association, since 2011.



From 2006 to 2014, he was an Assistant Lecturer with the Department of Communication Engineering, College of Electronics, University of Ninawah, Mosul, Iraq. His general research interests include emerging technologies for 5G wireless/mobile communication systems, including adaptive beamforming algorithms for wireless networks, multi-user massive MIMO, new modulation and waveform schemes, heterogeneous networks, and mmwave channel models.



**NAZAR T. ALI** (M'01–SM'03) received the Ph.D. degree in electrical and electronic engineering from the University of Bradford, U.K., in 1990. From 1990 to 2000, he held various positions at the University of Bradford, starting with the post-doctoral position, from 1990 to 1996, worked on European and U.K. funded projects. He covered many research areas, such as practical implementations of wireless and optical transceiver systems, nonlinear modeling of optical predistorters for laser diodes, and MIMIC realization of active inductors. He then became a Lecturer at the Department of Electrical and Electronic Engineering, University of Bradford. He was the Leader of radio frequency modules delivered to UG and PG students. He is currently an Associate Professor with Khalifa University, United Arab Emirates. He has published over 90 peer-reviewed conference and journal papers and one book chapter in *Broadband Antennas* (Springer, 2018). His current research interests include OFDM-based systems, indoor and outdoor localization techniques, radio frequency circuit design, antennas, signal processing for radar applications, and applications of machine learning in localization and radars. He is a Chartered Engineer at U.K.



**WAF A SHUAIEB** was born in Elbida, Libya. She received the B.Eng. degree in electronics and electrical engineering from Omar Al-mukhtar University, Al Bayda, in 2008, the M.Sc. degree in electrical and electronics engineering from Alexandria University, Egypt, in 2010, and the Ph.D. degree in electrical engineering from the University of Bradford, in 2018. She is currently pursuing the Ph.D. degree. She was an Assistant Lecturer with the Electronic Department, Omar Al-Mukhtar University. She has been a Research Student in the cryptography and use biometric traits in the generation of private keys in public cryptosystem, since 2012. Her research interests include direction of arrival, including location-based service methodologies, such as angle of arrival.



**RAMEEZ ASIF** was born in Lahore, Pakistan. He received the B.Eng. degree in electronics and computer engineering from the University of Delaware, Newark, DE, USA, in 2010, and the M.Sc. and Ph.D. degrees in electrical and electronics engineering from the University of Bradford, U.K., in 2012 and 2018, respectively. He has been a Radio Frequency Design Engineer with Visibility Asset Management Ltd., since 2016. He has contributed to several international journal articles and conference papers. His research interests include antennas, MIMO, wavelets, and defected ground antennas. He is a member of the University of Bradford Industrial Advisory Board. He has been a member of the Institution of Engineering and Technology, since 2011.



**RAED A. ABD-ALHAMEED** (M'02–SM'13) is currently a Professor of electromagnetic and radio frequency engineering with the University of Bradford, U.K. He is also the Leader of radio frequency, propagation, sensor design, and signal processing, in addition to leading the Communications Research Group, School of Engineering and Informatics, University of Bradford, for years. Since 2009, he has been a Research Visitor with Wrexham Glyndŵr University, U.K., covering the wireless and communications research areas. He has many years of research experience in the areas of radio frequency, signal processing, propagations, antennas, and electromagnetic computational techniques. He has published over 600 academic journal and conference papers. He is also a Principal Investigator for several funded applications to EPSRCs and the Leader of several successful knowledge transfer programmes, such as with Arris (previously known as Pace plc), Yorkshire Water plc, Harvard Engineering plc, IETG Ltd., Seven Technologies Group, Emkay Ltd., and TwoWorld Ltd. He has coauthored four books and several book chapters. His research interests include computational methods and optimizations, wireless and mobile communications, sensor design, EMC, beam steering antennas, energy-efficient PAs, and RF predistorter design applications. He is a Fellow of the Institution of Engineering and Technology and the Higher Education Academy. He was a recipient of the Business Innovation Award for his successful KTP with Pace and Datong companies on the design and implementation of MIMO sensor systems and antenna array design for service localizations. He is also the Chair of several successful workshops on energy-efficient and reconfigurable transceivers: Approach toward Energy Conservation and CO<sub>2</sub> Reduction that addresses the biggest challenges for the future wireless systems. He has also been a Co-Investigator of several funded research projects, including the H2020 Marie Skłodowska-Curie Actions: Innovative Training Networks Secure Network Coding for Next Generation Mobile Small Cells 5G-US, the Nonlinear and Demodulation Mechanisms in Biological Tissue (Department of Health, Mobile Telecommunications and Health Research Programme), and the Assessment of the Potential Direct Effects of Cellular Phones on the Nervous System (EU: collaboration with six other major research organizations across Europe). He has been the Guest Editor of *IET Science, Measurement & Technology* journal, since 2009. He is also a Chartered Engineer.



**OMAR OBEIDAT** received the B.Sc. degree in electrical engineering from the Jordan University of Science and Technology, in 2006, and the M.Sc. degree in wireless communication engineering from Al Yarmouk University, in 2009. He is currently pursuing the Ph.D. degree with Wayne State University. His research interests include non-destructive evaluation, thermal imaging, and indoor localization services.



**MOHAMMED S. A. BIN-MELHA** was born in Abha, Saudi Arabia. He received the B.Eng., M.Sc., and Ph.D. degrees in electrical engineering from the University of Bradford, U.K., in 2001, 2008, and 2013, respectively. He has extensive international working experience across the Civil Aviation Authority, from 1987 to 2015, and then, has been appointed at Saudi Air Navigation Services Company, in 2015. He has published several international conference and journals on design and model of antennas and various sensors. His research interests include the areas of electromagnetics and radio frequency engineering, with a particular focus on computational electromagnetics, RF sensor design, and antenna design, modeling, and deployment for surface and underground wireless sensor applications.



**PETER EXCELL** (M'80–LSM'14) received the B.Sc. degree in engineering science from the University of Reading, U.K., in 1970, and the Ph.D. degree for research in electromagnetic hazards from the University of Bradford, U.K., in 1980. He was with the University of Bradford, in 1971, and transferred to Wrexham Glyndŵr University, Wrexham, U.K., in 2007, retiring as the Deputy Vice-Chancellor, in 2015. He is currently a Professor Emeritus with Wrexham Glyndŵr University and a Visiting Professor with the University of Bradford. He has authored or coauthored over 500 publications. His long-standing research interest

includes the applications and computation of high-frequency electromagnetic fields. This led to significant advances in the development of the hybrid field computation method and novel designs for antennas. His current works include the studies of advanced methods for electromagnetic field computation (including the use of high-performance computing), the effect of electromagnetic fields on biological cells, advanced antenna designs for mobile communications, and consideration of usage scenarios for future mobile communications devices. He is a Fellow of the Institution of Engineering and Technology, the British Computer Society, and the Higher Education Academy, a Chartered Engineer and a Chartered IT Professional, and a member of the Association for Computing Machinery, the Applied Computational Electromagnetics Society, and the Bioelectromagnetics Society.

• • •